Molybdenum sulphides on carbon supports as electrocatalysts for hydrogen evolution in acidic industrial wastewater

M. Kokko[a,e], F. Bayerköhler[b], J. Erben[a], R. Zengerle[a,c,d], Ph. Kurz[b,*], S. Kerzenmacher[a,*]

[a] Laboratory for MEMS Applications, IMTEK – Department of Microsystems Engineering, University of Freiburg, Georges-Koehler-Allee 103, 79110 Freiburg, Germany

[b] Institute for Inorganic and Analytical Chemistry and Freiburg Materials Research Center, University of Freiburg, Albertstraße 21, 79104 Freiburg, Germany

[c] BIOSS – Centre for Biological Signalling Studies, University of Freiburg, 79110 Freiburg, Germany

[d] Hahn-Schickard, Georges-Koehler-Allee 103, 79110 Freiburg, Germany

[e] Present address: Department of Chemistry and Bioengineering, Tampere University of Technology, Tampere, Finland

* Corresponding authors: sven.kerzenmacher@imtek.de (S. Kerzenmacher), philipp.kurz@ac.uni-freiburg.de (Ph. Kurz)

Abstract

Microbial electrolysis cells (MECs) are an attractive future alternative technology to generate renewable hydrogen and simultaneously treat wastewaters. The thermodynamics of hydrogen evolution in MEC can be greatly improved by operating the cathode at acidic pH in combination with a neutral pH microbial anode. This can easily be achieved with acidic industrial wastewaters that have to be neutralised before discharge. For the hydrogen evolution reaction (HER) in acidic wastewater, efficient and inexpensive catalysts are required that are compatible with the often complex chemical composition of wastewaters. In this study, molybdenum sulphides (MoS_x) on different carbon supports were successfully used for hydrogen evolution in different acidic media. At first, the cathodes were screened by linear sweep voltammetry in sulphuric acid (pH 0) or phosphate buffer (pH 2.2). After this, the overpotentials for H_2 production of the best cathodes and their long term performances (≥1 week) were determined in acidic industrial wastewater (pH 2.4) obtained from a plant mainly producing cellulose acetate. For the most promising MoS_x cathodes, the overpotentials for HER (at 3 $mA \cdot cm^{-2}$) were only ~40 mV higher than for a platinum electrode. Most importantly, the catalytic efficiency of the MoS_x electrodes improved in the wastewater over time (7-17 days), while Pt electrodes were found to be slowly deactivated. Thus, MoS_x emerges as an affordable, efficient and especially durable electrocatalyst for HER in real acidic wastewaters that could take energy production from wastewaters in the form of hydrogen towards practical applications.

Keywords: hydrogen, industrial wastewater, microbial electrolysis cell, molybdenum sulphide

1. Introduction

Hydrogen, produced in a renewable way, is considered as a potential future energy carrier. While the majority of today´s hydrogen is still generated from fossil fuels by steam reforming, water electrolysis using renewable electricity (e.g. solar or wind power) is regarded as one of the key technologies for the sustainable production of hydrogen [1]. The energy required for hydrogen production through water electrolysis can be significantly lowered by choosing an alternative anode reaction that is thermodynamically more favorable than the oxygen evolution reaction. One such synergistic reaction is the bioelectrochemical oxidation of organic carbon (e.g. acetate) present in wastewaters by means of a microbial anode. Such systems with bacterial catalysts at the anode are called microbial electrolysis cells (MECs) and are currently being developed as an efficient technology to simultaneously treat wastewaters and produce hydrogen. In MECs, the biological oxidation of organic components at the anode (usually at neutral pH) produces the reducing equivalents used for H_2 evolution at the cathode, where the pH can range from 2 to 12.5 [2].
At neutral pH, the theoretical voltage difference required to drive the cathodic H_2 evolution reaction (HER) in combination with a microbial anode for acetate oxidation is only 0.11 V. This value is more than ten times lower compared to the theoretical minimum of 1.23 V required for the conventional electrolysis of water, where H_2 production at the cathode is coupled to anodic oxygen evolution. Furthermore, if an MEC is operated with a pH gradient between anode and cathode, the theoretically required voltage can be reduced by 59 mV for each pH unit that the acidic cathode deviates from neutral pH required at the microbial anode. While in theory a difference of two pH units between an acetate-oxidising anode and a hydrogen evolution cathode would be sufficient to drive the electrode reactions with zero voltage, irreversible losses occur and larger voltages are required partly due to overpotentials (η) at the cathode side.

Hydrogen production in an MEC with a pH difference between anode (pH 7) and cathode (pH 2) has previously been reported by Ruiz et al. [2]. However, their study was conducted with "laboratory electrolytes" that are not relevant to practical applications, where wastewater serves as electrolyte both at the anode and cathode chamber. The type and characteristics of the wastewater dictates the operational conditions at the cathode, and thus the overpotential of HER. It is therefore essential to develop efficient, durable, and affordable catalysts that decrease the overpotential of the HER under the conditions for practical relevance. The high cost of efficient cathode materials for HER is regarded as one of the main limiting factor in scaling-up of MECs [3].

In conventional water electrolysis cells, noble metals such as platinum are often used as HER catalysts. However, the excellent catalytic properties of platinum (η's close to 0 mV at some conditions [4,5]) come with a high cost of currently ~6800 US$·(mol Pt)$^{-1}$ (http://www.lme.com, accessed on 22.07.2016). In addition, the poisoning of Pt-based HER catalysts in MECs has been reported and might be caused by sulphide [6] or due to the adsorption of phosphate on the electrode surfaces [7]. In MECs, some alternative HER catalyst materials have been tested with real wastewaters as electrolytes, including stainless steel [8,9] and nickel [10,11]. However, stainless steel electrodes have high overpotentials and can also encounter poisoning [12] or corrosion [13]. Nickel catalysts have shown promising results for H_2 evolution at near neutral pH [14,15] but are not suitable for acidic pH values. There are no studies addressing HER in real wastewaters with acidic pH values.

Molybdenum sulphides (MoS_x) have recently gained attention due to their high catalytic activity for HER, their excellent chemical stability [16–18] and the very low cost of ~1.5 US$·$mol_{Mo}^{-1}$

(http://www.lme.com, accessed on 22.07.2016). Molybdenum sulphides can be generally described as ionic compounds containing Mo^{4+} cations and sulphide (S^{2-}) as well as disulphide (S_2^{2-}) anions. A simplified general formula $Mo^{IV}(S^{2-})_a(S_2^{2-})_b$ can be formulated for these materials, for example, with a = b = 1 in the case of amorphous MoS_3, i.e. $Mo^{IV}(S^{2-})(S_2^{2-})$ [19]. Additionally, the structural motif of Mo cations embedded in a sulphide-rich coordination sphere can also be found in the active site of the FeMo-nitrogenase enzyme, where the FeMoCo active site produces H_2 as a side-reaction while converting N_2 to NH_3 (for a review, see Laursen et al. [20]). For molybdenum sulphides, it has been shown that hydrogen atoms bind easily to sulphur anions at the edges of MoS_x-layers, where the HER reaction is thought to take place [5]. In MECs, electrodes with MoS_2 catalyst have been reported to have H_2 production rates comparable to Pt electrodes at neutral pH in synthetic medium, thus making molybdenum sulphide a promising catalysts for H_2 evolution [21].

However, MoS_x has two major limitations: 1) a low electric conductivity of the material and 2) a rather low number of active sites for HER catalysis [20–22]. To overcome these drawbacks, small MoS_x particles are often deposited on electrically conductive support materials by electrochemical deposition [23,24] or with the help of Nafion [25,26]. For MECs, MoS_x electrodes have been mainly prepared by mixing MoS_2 with Nafion and carbon black that is used to coat carbon cloth [12,27]. Nafion is, however, expensive, which might prevent its use in practical applications. Regarding the scaling-up of MECs, carbon based support materials such as carbon cloth are particularly attractive due to their low cost, sufficient electrical conductivity, and large specific surface area. Xia et al. [28] reported that the conductivity and current production capability of MoS_2 catalysts were affected by the concentration of MoS_2 on the electrode. In this way, the number of active sites and the material's conductivity could be improved, e.g., by increasing the number of electrodeposition

cycles [29] or by using suitable support materials, such as carbon nanotubes (CNTs) [30]. Thus, the electrode preparation process appears to be a very important step as it affects the composition, particle morphology and distribution of the MoS_x deposited on the electrode surface. In addition, it influences the costs of the manufactured MoS_x electrodes. Thus, novel ways to prepare MoS_x electrodes are required. MoS_x electrodes have already been widely studied for possible applications in conventional water electrolysis [5,28,30]. However, the requirements for MEC cathodes to operate in real wastewaters are different due to generally lower conductivities of the electrolytes and pH values deviating from the extremes commonly used in alkaline or acidic electrolysers. This difference in operation is compounded by the presence of various organic and sulphur-containing compounds that can compete for the electrons at the cathode or cause electrode poisoning.

The purpose of this study was to evaluate the use of MoS_x–based HER cathodes under application-relevant conditions in an acidic industrial wastewater. The major research question addressed is whether MoS_x-cathodes can sustain their high catalytic activity towards HER also in real acidic industrial wastewaters over extended periods of time. Furthermore, we investigated whether the H_2 production potentials under these conditions are affected by the electrode preparation method, since this will influence both cost and usability. Thereto different preparation methods for HER-cathodes composed of MoS_x as electrocatalyst and carbon materials as conducting supports were evaluated and their potential for HER were determined. Electrochemical hydrogen evolution by these MoS_x electrodes was first studied in sulphuric acid and phosphate buffer to screen for the most efficient cathodes and to compare their performances with earlier studies carried out under similar conditions. The best HER-cathodes from this screening were then investigated in real acidic

industrial wastewater obtained from a plant producing to a large part cellulose acetate. This cellulose derivative is produced worldwide on a large scale (especially for filter applications) by the reaction of acetic acid with cellulose, often in the presence of sulphuric acid acting as acetylation catalyst [31]. As a result, large amounts of acidic waste streams rich in acetic acid are available, which have to be neutralised at the industrial site before they can be discharged into a sewage system or wastewater treatment plant. Thus, near neutral wastewater fractions, rich in acetic acid is available for the anodic oxidation in a MEC, while the acidic wastewater could be used directly as electrolyte at the cathode to provide more thermodynamically favorable conditions for H_2 generation. To study the effects of the wastewater electrolyte on cathodic H_2 evolution, the cathodes prepared in this study were tested in half-cell experiments with abiotic anodes.

2. Materials and Methods

2.1 Chemicals and supporting carbon electrodes

Molybdenum sulphide (MoS_2 powder, < 2 μm) and ammonium tetrathio-molybdate ($(NH_4)_2[MoS_4]$) were purchased from Sigma Aldrich (Germany). Different carbon based electrodes, i.e. activated carbon cloth (ACC), buckypaper (BP) and electrospun carbon (ES), were used as support materials for MoS_x deposition. Activated carbon cloth (C-TEX 13) was purchased from MAST Carbon (Basingstoke, UK) and was used without pretreatment. For electrospinning, polyacrylonitrile powder (PAN) was dissolved in N'N-dimethylacetamide (DMAc, Sigma-Aldrich, Taufkirchen) by stirring at 70°C overnight. The electrospun materials were fabricated using a modified KatoTech (Kyoto, Japan) NEU electrospinning device (Fig. A.1). The modification allows hot-air assisted electrospinning as well as uniform fiber deposition on the collector. The material was spun from 13 wt% PAN (150,000 $g \cdot mol^{-1}$, Sigma-Aldrich) by applying a voltage of 16 kV, a polymer feed rate of 0.864 mL h^{-1}, a collector rotation of 2.5 m min^{-1}, and an airflow of 5 SCFH at 40°C. The electrospun PAN fiber mats were carbonized by heating first to 230°C in air and subsequently to 1100°C in N_2 atmosphere using a tube furnace (Gero, Germany).

Buckypaper electrodes were fabricated from multi-walled carbon nanotubes (MWCNTs) as described by Hussein et al. [32]. In short, 550 mg MWCNTs (Baytube C150 HP, Bayer Material Science AG, Germany) were dispersed in 1.1 L of a 1% aqueous solution of the surfactant Triton X-100 (Carl Roth, Germany), mixed for 15 min at 200-300 rpm and sonicated for 3 hours. The agglomerates of MWCNTs were removed from the solution by centrifugation at 2000 g for 15 min

and 135 mL of the MWCNT solution was vacuum-filtered on a nylon filter membrane (0.45 μm, Whatman, Maidstone, UK). The excess Triton was removed from the MWCNT film by several washing steps with water, isopropanol and acetone (for further information, see supplementary material of Kipf et al. [33]). After two days of washing (six washing steps) the buckypapers were dried at 70ºC overnight and weighed (MWCNT loading of 1.2 ± 0.2 mg cm^{-2}). For comparison, platinum/carbon electrodes (0.5 mg Pt cm^{-2}, i.e. 2.6 μmol cm^{-2}, Freudenberg H2315 I2C6, Quintech, Germany) and stainless steel electrodes (SS, SIKA-R1 AX, GKN, Germany) were used. Before the experiments, stainless steel electrodes were cleaned by sonication for 10 min each in acetone, isopropanol, and then twice in distilled water.

2.2 Electrode preparations

For a list of the different MoS_x-electrodes prepared for this study, see Table 1. Drop coating on supporting materials was carried out using a solution containing 1.5 mg MoS_2 in 1 mL ethanol and sonicated for 10 min. 130 μL of this suspension was drop-coated on the support material (1 cm^2) and heated at 80ºC overnight. The resulting loading was calculated to be 0.2 mg MoS_2 cm^{-2} (2.1 μmol cm^{-2}). In some experiments, ES and BP electrodes were acid treated with HCl (pH 5) for 30 min before drop-coating. Impregnation (drop coating) on acid treated supporting materials was done as described above with $(NH_4)_2MoS_4$ (concentration of MoS_2 in ethanol was 1.5 mg mL^{-1}) instead of MoS_2 followed by heat treatment. The resulting loading was calculated to be 0.2 mg MoS_2 cm^{-2} (2.1 μmol cm^{-2}). Electrodeposition on the three supporting materials was done with a method modified from Zhang et al. [34]. For this, the electrode was first soaked in electrolyte (0.05 M $(NH_4)_2MoS_4$ in 0.1 M KCl) for 15 min and simultaneously made anoxic by purging the

189 solution with N_2. The current density was then set to -8.3 mA cm^{-2} for 15 min to reductively deposit

190 $Mo^{IV}S_x$ from the soluble Mo^{VI} precursor. Fig. A.2 shows a typical cathode potential response.

191

192 **Table 1** Electrodes investigated in this study.

Electrode substrate (sample abbreviation)	**MoS_x precursor**	**Preparation method**
Activated carbon cloth (ACC)	-	-
Activated carbon cloth (ACC-ED)	$(NH_4)_2MoS_4$	Electrodeposition
Activated carbon cloth (ACC-DC)	MoS_2	Drop coating
Buckypaper (BP)	-	-
Buckypaper (BP-ED)	$(NH_4)_2MoS_4$	Electrodeposition
Buckypaper (BP-DC)	MoS_2	Drop coating
Buckypaper (BP-IHT)	$(NH_4)_2MoS_4$	Impregnation followed by heat treatment
Buckypaper (BP-MoS_2)	MoS_2	MoSx mixed with MWCNTs before buckypaper preparation
Electrospun carbon nanofibers (ES)	-	-
Electrospun carbon nanofibers (ES-ED)	$(NH_4)_2MoS_4$	Electrodeposition
Electrospun carbon nanofibers (ES-DC)	MoS_2	Drop coating
Electrospun carbon nanofibers (ES-IHT)	$(NH_4)_2MoS_4$	Impregnation followed by heat treatment
Electrospun carbon nanofibers (ES-MoS_2)	$(NH_4)_2MoS_4$	MoSx mixed with MWCNTs before buckypaper preparation

193 MWCNT = multi-walled carbon nanotubes

194

195 Buckypapers were also prepared by mixing 100 mg MoS_2 into the MWCNT / Triton mixture before

196 sonication. The buckypaper preparation procedure was otherwise the same as described above and

197 should result in MoS_2 loading of 0.2 mg cm^{-2} (2.1 μmol cm^{-2}). Electrospun electrodes were also

198 prepared by mixing MoS_2 (Sigma Aldrich) directly into the PAN/MDAc mixture used for the

199 electrospinning process. The material was then spun from 9 wt% PAN (200,000 g mol^{-1}, Dolan,

200 Germany) containing 0.24 wt% MoS_2 particles (Sigma-Aldrich, Taufkirchen, Germany) by applying

201 a voltage of 18.5 kV, a polymer feed rate of 0.864 ml h^{-1}, and a collector rotation of 9 m min^{-1}. The

following carbonization step was then carried out as described above. The resulting MoS_2 loading was calculated to be approximately 0.2 mg cm^{-2} (2.1 μmol cm^{-2}).

2.3 Electrochemical characterization

Linear sweep voltammetry (LSV) was used to test the activity of the modified electrodes (Table 1) towards HER in three electrolytes, i.e., 0.5 M H_2SO_4, 0.5 M phosphate buffer, and acidic industrial wastewater. The LSVs were used for comparing the electrodes and for the evaluation of MoS_x deposition methods and not to give absolute values - therefore only one repetition per modified electrode was carried out. The experiments were conducted at 30ºC and for each experiment a new electrode with working area of 1 cm^2 was used. The pH and conductivities of the electrolytes were as shown in Table 2 and the effects of different electrolytes on the LSV curves are shown in Fig. A.3. The acidic industrial wastewater had a chemical oxygen demand (COD) between 4.5 and 5.6 g L^{-1} (depending on the sampling time), from which 1.8-3.8 g L^{-1} (30-63 mmol L^{-1}) was organic acids (measured as acetic acid equivalents). In addition, the wastewater contained 2.0-2.8 g L^{-1} (21-29 mmol L^{-1}) sulphate.

LSVs were measured in a three-electrode setup where the modified electrode was the working electrode, a Pt mesh (Goodfellow, Germany) acted as counter electrode and a saturated calomel electrode (SCE, +0.244 V vs. SHE, KE 11, Sensortechnik Meinsberg, Germany) as reference electrode. The electrodes were connected by titanium wires and a Solatron 1470E potentiostat (Ametek, Farnborough, UK) was used to record LSVs from open circuit voltage (OCV) +20 mV to

-1.20 V (vs. SCE), which were repeated three times for each electrode. Before starting the experiments, the electrolyte was made anoxic by N_2 purging for 15 min.

Table 2 Characteristics of the three electrolytes used for LSV experiments.

Electrolyte	pH	Conductivity (mS cm^{-1})	Theoretical H_2 evolution starts at (mV vs. SCE)
0.5 M H_2SO_4	0.2	200	-241
0.5 M phosphate buffer	2.2	38	-368
Industrial wastewater	2.4 ± 0.2	6.1 ± 0.6	-380

The LSV results were corrected for the ohmic potential drop (iR, uncompensated resistance), which was analysed with a current interrupt method in phosphate buffer and industrial wastewater. In this method, untreated electrodes (1 cm^2) were placed in the different electrolytes using the three-electrode set-up described above. A current of 1 mA was applied for 4 s with a potentiostat (PCI4/300 Model, Gamry Systems, Pennsylvania) that enables a small sampling period of 60 μs. The voltage drop upon current interruption was measured and used for calculating the ohmic potential drop. The mean iR values (± standard deviation) for 0.5 M phosphate buffer and acidic industrial wastewater were 89±8 Ω and 240±8 Ω, respectively. For measuring the uncompensated resistance in 0.5 M H_2SO_4, the LSVs were run in the three electrode set-up by placing the reference electrode with a Luggin capillary in front of the electrode or to its normal position. The ohmic resistance between these two runs were measured from the linear regions of the LSV curves and the difference was regarded as the ohmic potential drop. The thus obtained iR values were 0.01 Ω, 5.7 Ω, 9.9 Ω and 7.5 Ω for ACC, BP, ES and Pt electrodes, respectively.

In each case, the third run of the LSVs was used to compare the results. All the potentials are reported against RHE, if not otherwise mentioned (U (V vs. RHE) = U (V vs. SCE) + 0.244 V + 0.058 V*pH). Electrode performances were compared by determining the onset overpotentials by drawing a tangent on the linear region of the LSV curve and reading the cathode potential at 0 mA cm^{-2}. Furthermore, the overpotentials were determined at current densities of 1, 2 and 10 mA cm^{-2} as described by Wirth et al. [35]. Tafel slopes were calculated for the electrodes run in 0.5 M H_2SO_4 to estimate the hydrogen evolution reaction (HER) mechanisms. The onset overpotential and overpotential results were rounded to 10 mV.

2.4 Long term experiments

The long term behaviour of the most promising electrodes was determined by applying a constant reductive current of 3 mA cm^{-2} for three parallel electrodes for at least one week or as long as the cathode potential was stable (change in cathode potential < 5 mV d^{-1}). The experiments were conducted in a 6-electrode set-up that had a working volume of 1 L [36]. In this reactor, six half-cell cathodes (1 cm^2) can be characterised simultaneously. Again, Pt meshes were used as counter electrodes and SCE as reference electrode. The working and counter electrodes were connected with Ti wires. As electrolyte, 0.5 M phosphate buffer or acidic industrial wastewater was used and was continuously purged with humidified N_2 to ensure anoxic conditions. The current was applied with an electrical testing system consisting of an electronic load (STG 2008 stimulus generator, Multichannel Systems, Germany) to apply the chosen current, and a data acquisition unit (Keithley 2700, Keithley, Germering, Germany) to record the cathode potentials against the reference electrodes [36]. The experiments were conducted at 30°C. The results were corrected for

uncompensated resistance as determined by numerical simulation (COMSOL) according to the used reactor geometry and the position of the electrodes (reference, working and counter electrode) using the conductivities of the phosphate buffer (19 mS cm^{-1}) and wastewater (6.35 mS cm^{-1}). The mean iR values in phosphate buffer and industrial wastewater were 55 ± 2 Ω and 165 ± 5 Ω, respectively. In both electrolytes, the pH changes in long term experiments were less than 0.05 pH units over the entire time of the experiments.

2.5 Hydrogen production yields

The hydrogen production yields of BP-ED and BP-IHT electrodes were determined in two-chamber electrochemical cells with abiotic anodes as counter electrodes. The anode and cathode chambers had total and working volumes of 53 and 40 mL, respectively. The compartments were separated with an anion exchange membrane (fumasep FAA-PK-130, Fumatech, Germany) and reference electrode (SCE, +0.244 V vs. SHE, KE 11, Sensortechnik Meinsberg, Germany) was separated from the cathode compartment with a proton exchange membrane (fumapem F-950, Fumatech, Germany). Each experiment was conducted with a fresh MoS_x electrode that had a working area of 1 cm^2 and two parallel reactors were run for each set of parameters. Pt mesh was used as counter electrode at the anode. Both anode and cathode compartments contained acidic industrial wastewater (Table 2) and were made anoxic by purging them with N_2 for at least 15 min prior to the start of the experiments. To keep the pH stable, fresh anoxic wastewater was pumped to both compartments with a flow rate of 58 μL min^{-1} resulting in a hydraulic retention time of 11.6 h. The cathode potential was set to -1.2 V vs. SCE (-0.82 V vs. RHE) with a potentiostat (PCI4/300. Gamry Instruments) and the current was measured. The gases produced were collected into 0.1 L gas-bags

289 (Calibrated Instruments, USA) for 1 week. The wastewater characteristics (pH, conductivity) at the
290 cathode and anode were analysed in the beginning and in the end of the experiment. The cathodic
291 hydrogen recoveries were calculated as suggested by Logan et al. [6].
292
293 **2.6 Chemical analyses and electrode characterisation**
294
295 Conductivity and pH were measured with inoLab® Multi 720 (WTW) instrument equipped with
296 TetraCon®325 conductivity probe (WTW) and SenTix®61 pH electrode (WTW). Organic acids,
297 chemical oxygen demand (COD) and sulphate in the wastewater were measured with cuvette tests
298 for organic acids (LCK365, Organic Acids Cuvette Test 50-2500 mg L^{-1}, Hach Lange, Germany),
299 COD (LCK514, Chemical Oxygen Demand test, 100-2000 mg L^{-1}, Hach Lange) and sulphate
300 (LCK153, Sulphate Cuvette Test 40-150 mg L^{-1}, Hach Lange). The gas composition in the gas bags
301 was analysed using a gas chromatograph (Clarus 480, PerkinElmer) equipped with 5 Å molecular
302 sieve column (Restek) and a thermal conductivity detector (TCD). The temperatures of oven,
303 injector and detector were 70°C, 100°C and 280°C, respectively. Argon was used as carrier gas at a
304 pressure of 290 kPa. The volume of the gas in the gas bags was analysed with a water displacement
305 method.
306
307 The electrode surfaces were imaged with a scanning electron microscope (SEM, Zeiss Supra 60 VP)
308 with a working distance of 10 mm and acceleration voltage of 5 kV. Energy-dispersive X-ray
309 (EDX) spectra were used to determine the sulphur-to-molybdenum ratios for the catalyst layers with
310 an Oxford Instruments Inca 300 EDX. For each electrode, five spots were chosen for EDX
311 measurements and an average S:Mo-ratio was calculated from the five recorded EDX spectra.

3. Results and Discussion

3.1 Electrode preparation

For the fabrication of MoS_x-coated carbon electrodes, three materials were used as carbon supports for the deposition of molybdenum sulphides (MoS_x): activated carbon cloth (ACC), electrospun carbon (ES) and buckypaper (BP) (Fig. 1, Table 1). Furthermore, three different deposition methods that can be realised at moderate temperatures were chosen. Overall, a screening on the effects of both the carbon supports and the MoS_x deposition methods was then carried out to study the influence of both parameters on the electrocatalytic activity towards HER.

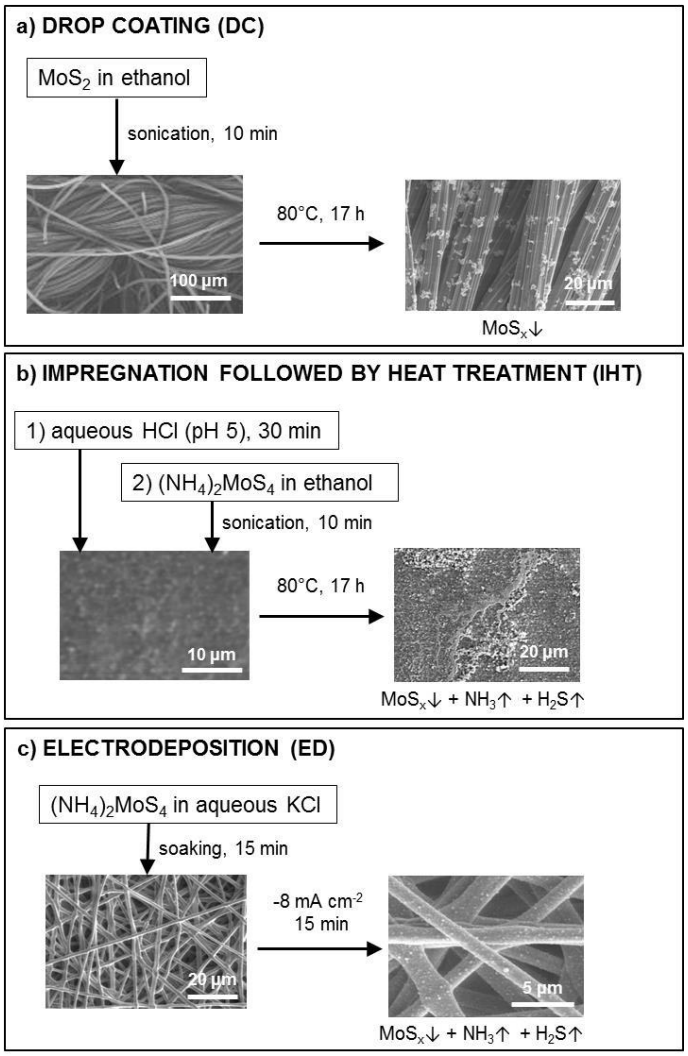

Figure 1 Schematic illustration of deposition of MoS_x a) on activated carbon cloth (ACC) with drop coating (DC), b) on buckypaper (BP) electrode with impregnation followed by heat treatment (IHT), and c) on electrospun (ES) carbon nanofibers with electrodeposition (ED).

3.2 Electrode characterization

SEM micrographs of the electrodes after MoS_x deposition are shown in Fig. 2. In combination with scanning electron microscopy (SEM), the samples were also analysed by energy dispersive X-ray spectroscopy (EDX) to estimate the S : Mo ratio for each sample (Fig. 2). The large standard

deviations of the EDX results (up to ±0.9) in these cases can be attributed either to the chemical reactions on the electrode surfaces (resulting in $Mo^{IV}(S^{2-})_a(S_2^{2-})_b$ materials of variable a : b-ratios) or to a large measurement uncertainty, as comparably small amounts of MoS_x were present on a large background of carbon. Drop coating with MoS_2 resulted in agglomerated particles (< 1 μm) on the electrode surface, while the distribution of the particles was uneven. The ratio of S to Mo in the drop coated electrodes was in the range of 2.3 and 2.6 (Fig. 2.A, B, E), which is higher than the S : Mo –ratio of 2.0 of the commercial MoS_2 used. Impregnation of ES and BP electrodes with solutions of $(NH_4)_2MoS_4$ in ethanol followed by mild heat treatment (80°C, 17 h) resulted in smaller particles covering the electrodes with S : Mo ratios of 2.6 and 3.3, respectively (Fig. 2.C,D). According to Li et al. [5], heating a mixture of diluted HCl (pH5) and $(NH_4)_2MoS_4$ on CNTs at 90°C results in electrostatic interactions leading to the adsorption of thiomolybdate on the CNTs. This then decomposes into amorphous MoS_x at 90°C. Li et al. [5] also treated N-doped CNT (NCNT) or plain CNT forest with acid followed by addition of $(NH_4)_2MoS_4$ and heating the mixture to 90°C. They observed that NCNTs were coated with amorphous MoS_3 including tiny MoS_2 crystalline domains that were in close contact with the NCNT surface, while the CNT surface contained infrequently deposited MoS_2 patches. In our study, the electrodes seemed to contain both tiny particles and patches, when carbon supports were impregnated with $(NH_4)_2MoS_4$ and heat treated (Fig. 2.C, D).

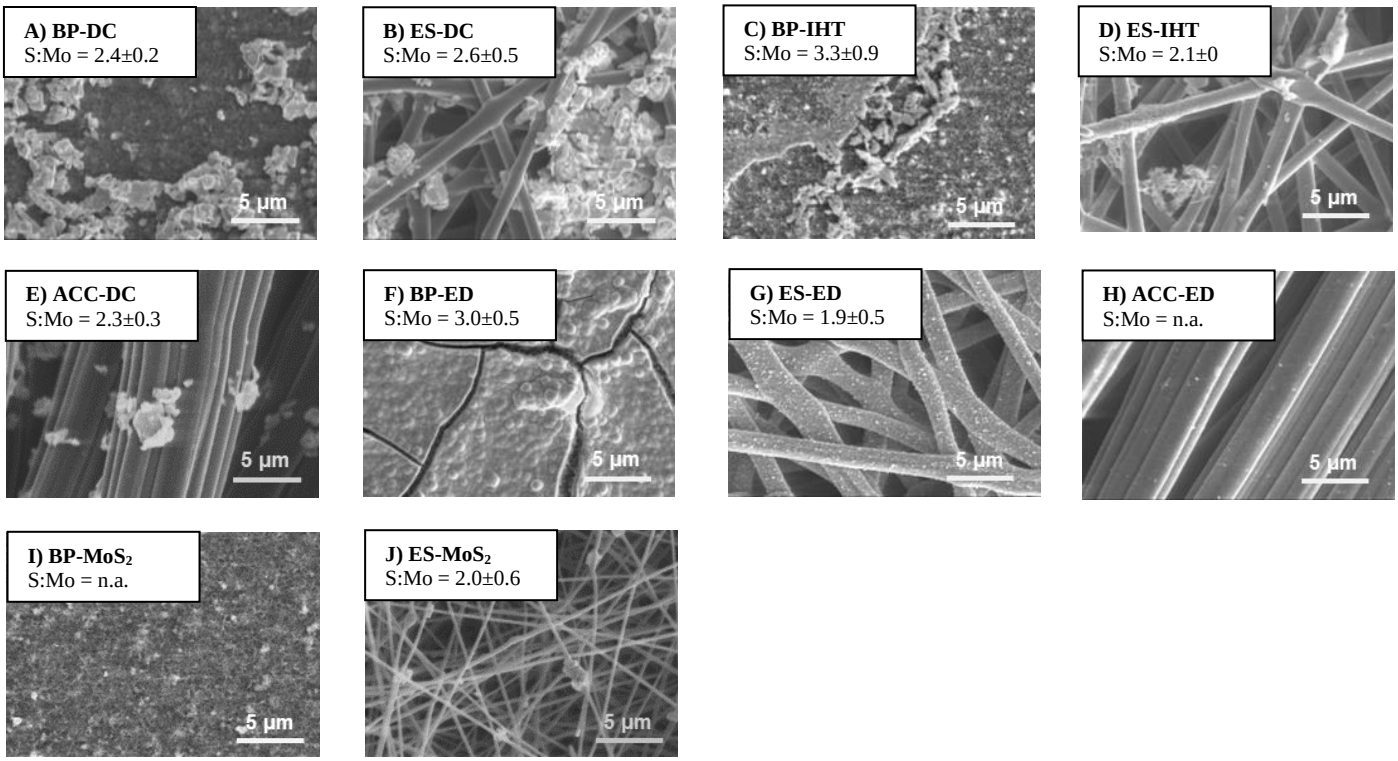

Figure 2 SEM pictures and EDX data (ratio of sulphur to molybdenum) for electrodes prepared by different routes for depositing MoS_x on various carbon supports. For abbreviations, see Table 1. n.a.: below the EDX detection limit.

Electrodeposition on ES and ACC electrodes resulted in an even coverage of small MoS_2 particles on the electrode material (Fig. 2.G, H). Electrodeposition on the BP electrode, on the other hand, resulted in a cracked mat built up mainly from MoS_3 that contained spherical formations (Fig. 2.F). The different molybdenum sulphide layers on the BP electrodes likely resulted from the flatter structure of the BP support (which also contains very small pores in the range of 50 nm [32]). It is likely that the same amount of MoS_2 was electrodeposited on the surfaces of BP, ES and ACC electrodes. However, as BP has a smaller accessible surface area, a layer of MoS_3 formed on top of the BP electrode instead of an even distribution of the particles. Zhang et al. [34] obtained MoS_x nanoparticles of 40-90 nm on carbon nanotube films with the same electrodeposition method.

However, in their study the CNTs were vertically aligned and thus provided a surface area that's more accessible for MoS_2 deposition. Mixing MoS_2 to the polymer before preparation of ES electrodes resulted in electrodes mainly covered by MoS_2 particles (Fig. 2.J). EDX results could not be obtained for ACC-ED and BP-MoS_2 electrodes due to the low amount of Mo and S compared to carbon.

Deposition of MoS_x on carbon supports resulted in S : Mo ratios varying from 1.9 to 3.3. These differences likely occur due to variations of the sulphide-to-disulphide ratio in the MoS_x materials (general formula $Mo^{IV}(S^{2-})_a(S_2^{2-})_b$). Thus, the higher the S : Mo ratio, the more sulphur is present in the MoS_x in the form of S_2^{2-}. Since hydrogen atoms are known to bind to the disulphide edges of the MoS_x particles during catalysis [37], higher S : Mo-ratios are most likely beneficial for HER catalysis. In the sample set studied here, both the MoS_x morphology and the S : Mo-ratio seem to depend on the deposition method as well as the carbon support. For example, electrodeposition or impregnation followed by heat treatment resulted mainly in MoS_2 deposition on activated carbon cloth and electrospun electrodes, while buckypapers were coated mainly by a MoS_3 type compound by these treatment methods.

3.3 Catalytic activity towards HER in sulphuric acid

As an initial screening, the electrocatalytic HER activity of each electrode was first determined by recording linear sweep voltammograms (LSV) in 0.5 M H_2SO_4 (Fig. 3, Fig. A.4). This enabled us to compare our results with literature data on the performance of MoS_x electrodes in traditional water electrolysis.

The onset overpotentials for HER were determined by drawing a tangent on the linear region of the LSV curve and extrapolating it towards a current density of 0 mA cm^{-2} (Fig. A.5). In addition, the overpotentials were taken from the LSV data at fixed reductive current densities of 1, 2 and/or 10 mA cm^{-2}. As expected, the Pt electrode showed the best performance (Fig. 3) with an onset overpotential of only 20 mV. The overpotentials of the Pt electrode could not be determined at low reductive current densities due to capacitive behaviour of the electrode (Fig. A.5).

For almost all carbon electrodes the deposition of MoS_x increased the catalytic activity for H_2 evolution compared to untreated electrodes. The only exception was the activated carbon cloth electrode which had a lower onset overpotential (20 mV) than ACC electrodes coated with MoS_x by electrodeposition (40 mV) or drop coating (50 mV). The activity of the untreated ACC electrode for HER was further studied by applying a constant reductive current of 3 mA cm^{-2} for triplicate electrodes in 0.5 M H_2SO_4 for a longer time (Fig. A.6). It was observed that the overpotential of the ACC electrodes increased in the first hour from negative values to around 350 mV. This suggests that in the first hour some oxidised surface sites of the activated carbon cloth were reduced. This could explain the initially small "overpotentials" of untreated ACC electrodes, but the detected currents then actually do not represent proton but carbon reduction. After one week, the overpotentials of the untreated ACC electrodes had risen to around 200 mV. Hydrogen evolution with activated carbon cloths (VITO-CoRE™ and VITO-CASE™), has been earlier reported in phosphate buffer at pH 7 [38].

411 Drop coating of commercial MoS_2 on BP and ES electrodes also resulted in a lower HER activity
412 compared to untreated electrodes. Overall, these results indicate that drop coating with MoS_2 as
413 electrode treatment is not a suitable method to prepare HER-cathodes based on the studied carbon
414 supports, while the other electrode treatment methods should be further studied (Fig. 3). Especially,
415 other electrode treatments than drop coating often result in smaller MoS_x particle sizes, which
416 increases the specific surface areas and amount of sulphur edges and results in high catalytic activity
417 towards HER [16] compared to electrodes prepared by drop coating.
418

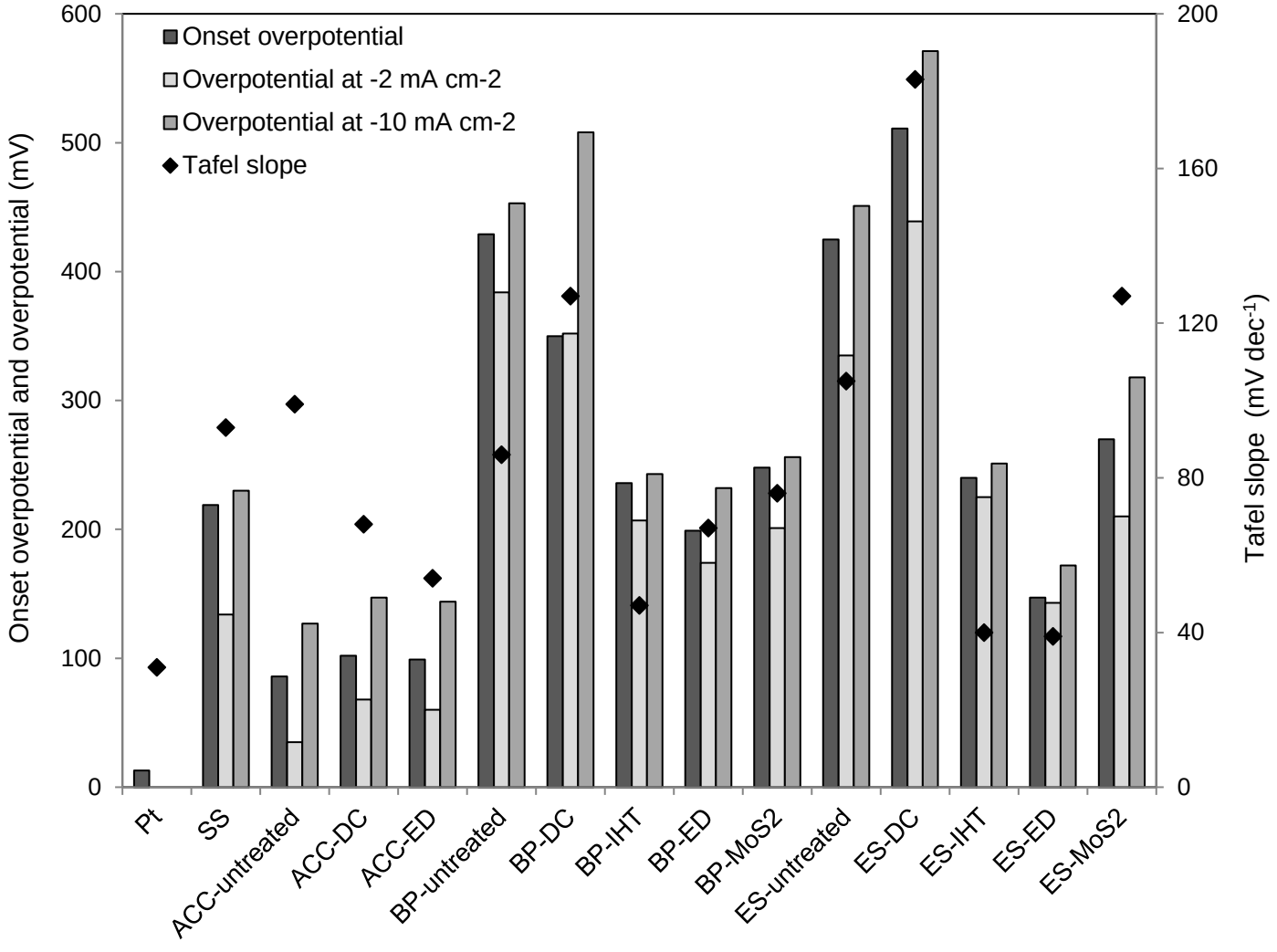

419

Figure 3 LSV results obtained in 0.5 M H_2SO_4 (for the abbreviations see Table 1).

In sulphuric acid, electrospun carbon with electrodeposited MoS_x (ES-ED) showed the lowest HER-onset overpotential of 150 mV and overpotential of 170 mV at 10 mA cm^{-2} of all studied MoS_x electrodes (Fig. 3). These results are lower than the values of stainless steel (220 and 230 mV, respectively), a material often used as cathode in MECs. The results were further compared to results reported in the literature for MoS_x electrodes in strongly acidic electrolytes (Table 3). Onset overpotentials and overpotentials obtained in this study are typical for MoS_x deposited on electrospun carbon, CNT and graphene electrodes. The good performance of the best electrodes in this study can likely be attributed to the good conductivity and large surface area of the carbon supports [28,30] as well as the good contact between MoS_x and the base material. The performance of the MoS_x electrodes could be further improved by optimizing the MoS_x-loading per area [28]. As MoS_x materials are typically poor conductors, the electrical accessibility of the electrode surface decreases with increasing thickness of the MoS_x-layer. Thus, too high MoS_x loadings should be avoided. The results indicate that the electrodes prepared for this study are comparable to MoS_x electrodes prepared previously for traditional electrolysis and that our cathodes also generally show a high catalytic activity towards HER.

Table 3 Comparison of the onset overpotentials, overpotentials and Tafel slopes obtained in this study to other MoS_x / carbon electrodes run in H_2SO_4. For the abbreviations of this study, see Table 1. The results obtained in this study were rounded to ten.

Electrode	Electrolyte	Onset overpotential (mV)	Overpotential (mV)		Tafel slope (mV dec^{-1})	Reference
Molybdenum carbide	0.1 M H_2SO_4	333	629	at 20 mA cm^{-2}	-	[35]
MoS_3 on GCE (CV)	pH 0	-	150	at 0.4 mA cm^{-2}	40	[29]
MoS_2-MWCNT on GCE	1 M H_2SO_4	250	500	at 30 mA cm^{-2}	-	[28]
MoS_2-MC on GCE		200	500	at 16 mA cm^{-2}		
MoS_2-RGO on GCE		130	500	at 235 mA cm^{-2}		
MoS_x-graphene (electro-deposition on GCE)	0.5M H_2SO_4	130	183	at 10 mA cm^{-2}	43	[24]
MoS_2 on GCE	0.5 M H_2SO_4	130	300	at 13.8 mA cm^{-2}	52	[39]
MoS_3-MWCNT drop coated on Ag electrode	1 M H_2SO_4	-	150	at 1.1 mA cm^{-2}	40	[40]
			200	at 10.8 mA cm^{-2}		
MoS_x/NCNT	0.5 M H_2SO_4	75	110	at 10 mA cm^{-2}	40	[5]
S rich-MoS_2-NCNF	0.5 M H_2SO_4	30	120	at 10 mA cm^{-2}	38	[41]
MoS_2-NCNF		98	230			
MoS_2/CNT	0.5 M H_2SO_4	90	-	-	44.6	[30]
MoS_2-RGO on GCE	0.5 M H_2SO_4	100	-	-	41	[4]
MoS_3 electrodeposited on GCE	1 M H_2SO_4	-	170	at 20 mA cm^{-2}	-	[23]
ACC	0.5 M H_2SO_4	90	130	at 10 mA cm^{-2}	100	This study
ACC-ED		100	140		50	
BP-IHT		240	240		50	
BP-ED		200	230		70	
ES-IHT		240	250		40	
ES-ED		150	170		40	

GCE = glassy carbon electrode, MWCNT = multi-walled carbon nanotubes, NCNF = N-doped carbon nanofibers, NCNT = N-doped carbon nanotubes, RGO = reduced graphene oxide

The Tafel slopes accessible from the LSV curves can be used to obtain information about the HER mechanism in acidic solution (Fig. 3). The smaller the Tafel slope, the faster the increase in H_2 production rate when the cathode overpotential is increased [39]. Three elementary reactions are thought to be involved in H_2 evolution in acidic conditions: the Volmer (Eq. 1), Heyrovsky (Eq. 2) and Tafel (Eq. 3) steps [20]. For Tafel slopes around 120 mV dec^{-1} or higher, the Volmer step is considered to be rate limiting [21]. Thus, the adsorption of hydrogen atoms on the cathode surface seems to be rate limiting for untreated ACC and ES, drop coated BP and ES, and ES-MoS_2. Limitations in the Volmer step might be due to a limited number of sulphur edges of the MoS_x particles [16] or poor electrical contact between MoS_x and the carbon support [21]. The Heyrovsky and Tafel steps proceed theoretically with Tafel slopes of 40 and 30 mV dec^{-1}, respectively [21]. Thus, HER with Pt electrode proceeds via the Volmer-Tafel mechanism with desorption (Tafel) as the limiting step, which is in agreement with the literature [5,24]. The Volmer-Heyrovsky mechanism, on the other hand, seems to be important for the following electrodes: BP-IHT, ES-IHT and ES-ED. With these electrodes, H-H bond formation and desorption of the H_2 product is likely limiting the H_2 evolution. Similarly, low Tafel slopes close to 40 mV dec^{-1} have also been reported for MoS_x electrodeposited on glassy carbon electrodes [24,29].

$$H_3O^+ + e^- \rightarrow H_{ad} + H_2O \quad (1)$$

$$H_3O^+ + H_{ad} + e^- \rightarrow H_2 + H_2O \quad (2)$$

$$2\ H_{ad} \rightarrow H_2 \quad (3)$$

Based on the Tafel slopes as well as the LSV results, electrodepositions (ED) or impregnations followed by heat treatment (IHT) result in the highest activity towards HER. The good performance of these electrodes can be attributed to small, highly dispersed MoS_x particles on the carbon electrodes ensuring strong electronic coupling of these two [4]. Drop coating did not seem to be an effective way to prepare MoS_x-electrodes for HER. In addition, the Tafel slope of untreated ACC electrodes was higher (100 mV) than that of other electrodes which resulted in low onset overpotentials and overpotentials. This suggests that despite the low onset overpotential and low overpotentials of ACC electrodes, a different mechanism for H_2 production is of importance here and this support material might not be the most attractive option for H_2 evolution.

3.4 Catalytic activity towards HER in phosphate buffer

Next, the catalytic activity of the MoS_x-coated electrodes towards HER was examined at pH 2.2 in 0.5 M phosphate buffer to mimic the pH regime of acidic industrial wastewaters and to identify the best-performing electrodes in this pH regime (Fig. 4, Fig. A.7). In phosphate buffer, the lowest onset overpotential of 20 mV was again observed for the Pt electrode. However, the LSV curve of Pt featured two distinctive waves (Fig. A.5b) that might result from the deprotonation of two different phosphate species (H_3PO_4 and $H_2PO_4^-$) at the electrode surface providing protons for H_2 evolution [7]. Due to these current steps, a determination of the overpotential for 2 mA cm^{-2} was not possible. The performance of the other reference material, stainless steel, was much poorer in the H_3PO_4 electrolyte compared to the previous runs in H_2SO_4 and resulted in higher overpotentials than for all the other electrodes tested (Fig. 4). Only

the untreated ACC support performed even worse and was found to be nearly inactive for HER in phosphate buffer. Among the MoS_x-electrodes, those modified with electrodeposition resulted in the lowest onset overpotentials of 20, 100 and 110 mV with BP-ED, ES-ED and ACC-ED, respectively. In phosphate buffer, the performance of the BP or ES electrodes modified with impregnation followed by heat treatment or constructed by mixing MoS_2 with MWCNTs or to the polymer, respectively, was similar.

In summary, the seemingly minor shift from the H_2SO_4 (pH 0) to an H_3PO_4 (pH 2.2) electrolyte resulted in major differences of the relative electrocatalytic HER-activities for the different electrode materials: a) in general, overpotentials increase (most likely due to the reduced proton availability), b) the performance of uncoated carbon or steel supports decreases substantially, and – most importantly – c) the differences between the platinum reference and the best MoS_x-electrodes narrows significantly.

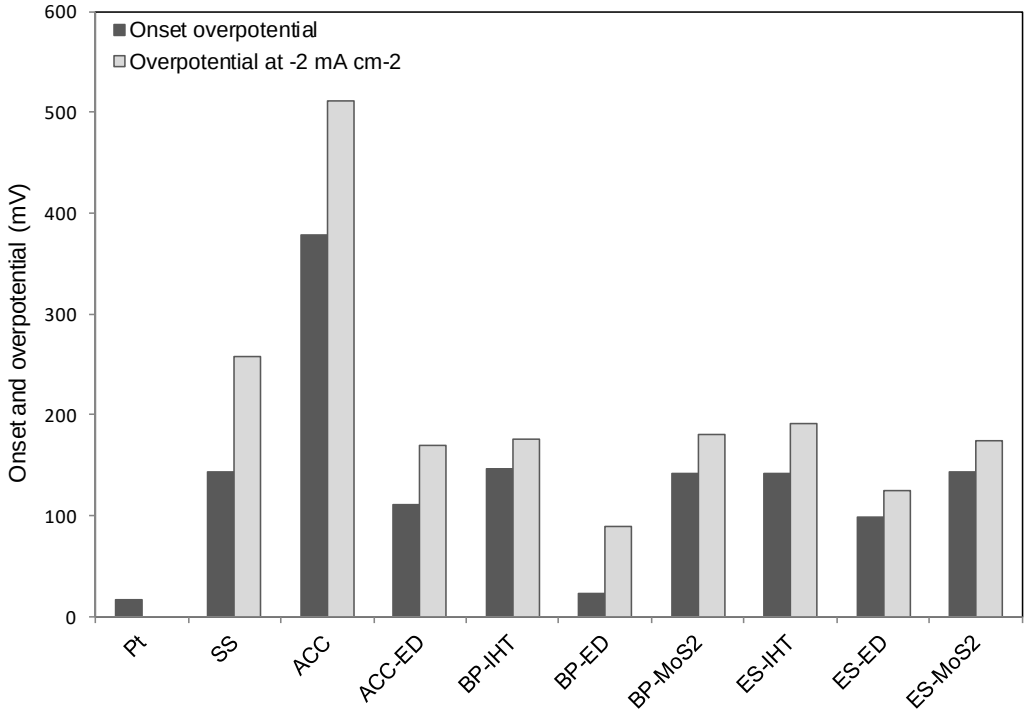

Figure 4 LSV results obtained in 0.5 M phosphate buffer, pH 2.2 (for the abbreviations see Table 1).

3.5 Catalytic activity towards HER in industrial wastewater

After establishing some basic HER-performance parameters for the well-defined, acidic H_2SO_4 and H_3PO_4 electrolytes, the electrocatalytic behaviour of the MoS_x-cathodes for HER was investigated in real industrial wastewater from a plant producing to a large part cellulose acetate. This wastewater had a pH of 2.4 and contained sulphate and acetate at concentrations of 20-30 mM and 30-60 mM, respectively. Additionally, the wastewater contains significant amounts of organic compounds due to the acid treatment of cellulose during the production process.

513 The onset overpotentials of the BP and ES electrodes with electrodeposited MoS_x in this
514 wastewater were 130 and 100 mV, respectively (Fig. 5, Fig. A.8) and thus only ~100 mV higher
515 than the onset overpotential of Pt (20 mV) and clearly lower than that of stainless steel
516 (190 mV). Tenca et al. [27] also reported that MoS_2 is a better catalyst for H_2 evolution than
517 stainless steel in industrial or food processing wastewaters at neutral pH. In addition, the
518 overpotentials needed for a reductive current density of 2 mA cm^{-2} for MoS_x-electrodes prepared
519 by electrodeposition were only 40 mV (BP-ED) or 60 mV (ES-ED) higher than that for the Pt
520 electrode. In addition to electrodes modified by electrodeposition, low overpotentials were also
521 detected for BP and ES electrodes where MoS_x was deposited via impregnation followed by heat
522 treatment, which causes the release of ammonia and sulphur from the $(NH_4)_2MoS_4$ precursor.
523 This step is often performed at temperatures of 200°C [4], but in the present study milder
524 conditions of only 80°C were sufficient to obtain good catalyst layers. From the different
525 electrodes the ones with MoS_x coating on buckypaper (BP) as support material (i.e. BP-MoS_2,
526 BP-IHT and BP-ED) were chosen for the long term experiments after an analysis of the
527 corresponding LSV curves (see Fig. 5 and Fig. A.9).
528
529 When comparing the results for acidic wastewater with the “laboratory electrolytes”, the HER-
530 overpotentials generally increased in the order: sulphuric acid < phosphoric acid < industrial
531 wastewater. The order is, as expected, reversed when comparing current densities: H_2SO_4 >
532 H_3PO_4 > industrial wastewater. Since the results have been corrected for the uncompensated
533 resistance, the variations cannot be explained by differences in conductivity alone. Instead, the
534 catalytic activities of the electrodes for HER in different electrolytes likely vary due to different

535 H_2 evolution reaction mechanisms and/or due to the reduction of compounds other than protons,

536 such as wastewater components.

537

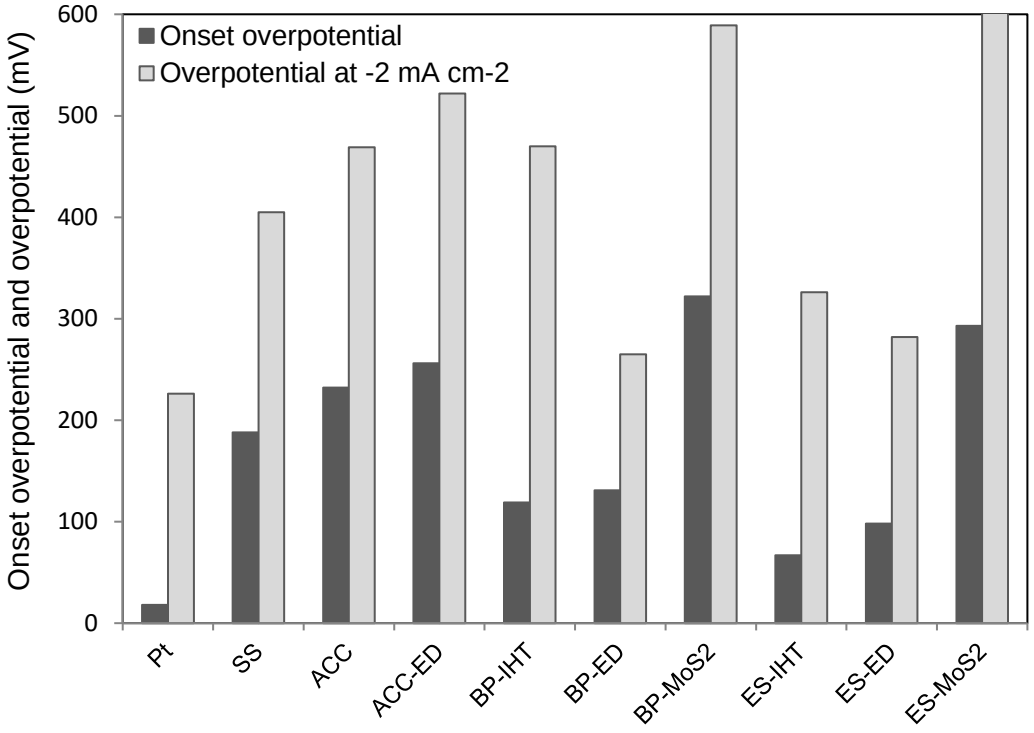

538

539 **Figure 5** LSV results obtained in acidic industrial wastewater, pH 2.4 (for the abbreviations see

540 Table 1).

541

542 **3.6 Long term H_2 evolution from the acidic wastewater electrolyte**

543

544 For long term experiments, Pt and selected buckypaper electrodes were run in

545 chronopotentiometry mode at reductive currents of 3 mA cm^{-2} in 0.5 M phosphate buffer or in

546 acidic industrial wastewater for extended time periods (1 - 2.5 weeks) until the cathode potential

547 had stabilised ($\Delta E < 5$ mV d^{-1}). The changes of cathode potentials against time for Pt and BP-

548 IHT electrodes and the overall results from stable operational period are plotted in Fig. 6 and
549 A.10 and in Fig. 7, respectively.
550
551 In phosphate buffer (Fig. 7), the overpotentials for BP-IHT and BP-MoS_2 electrodes surprisingly
552 decreased significantly over time from 220 ± 20 mV to 70 ± 20 mV and from 470 ± 60 mV to
553 260 ± 20 mV, respectively, while for BP-ED electrodes the overpotentials increased from 120 ±
554 10 mV to 190 ± 20 mV. The overpotentials of Pt decreased from -55 ± 15 to -81 ± 6 mV during
555 the run. The negative overpotentials for Pt electrodes are likely due to a special H_2 evolution
556 mechanism for Pt electrodes in phosphate buffer. Already the LSVs in phosphate buffer
557 indicated that phosphate species seemed to be able to adsorb onto the platinum surface donating
558 protons for H_2 production (Fig. A.5b). This would result in a lower local pH at the electrode
559 surface and affect the cathode potentials in long term.
560
561
562

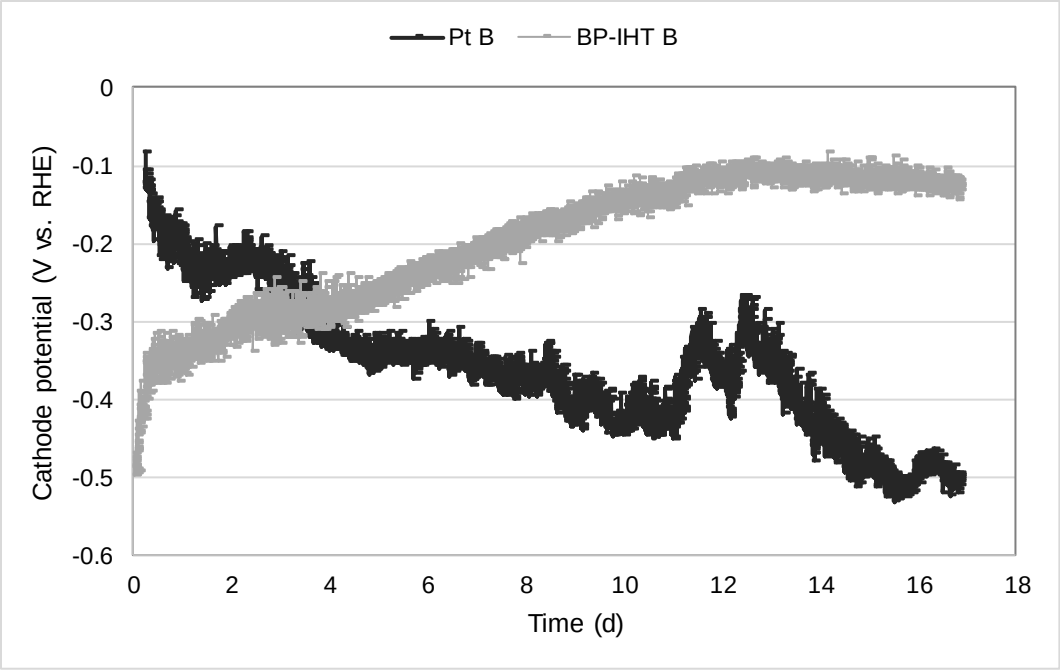

563

564 **Figure 6** Long term experimental run at reductive current of 3 mA cm^{-2} with Pt and BP-IHT

565 electrodes in real acidic industrial wastewater. The figure shows one of the three parallel

566 electrodes and the results have been corrected for uncompensated resistance. For all parallel

567 results, see Fig. A.10.

568

569

570

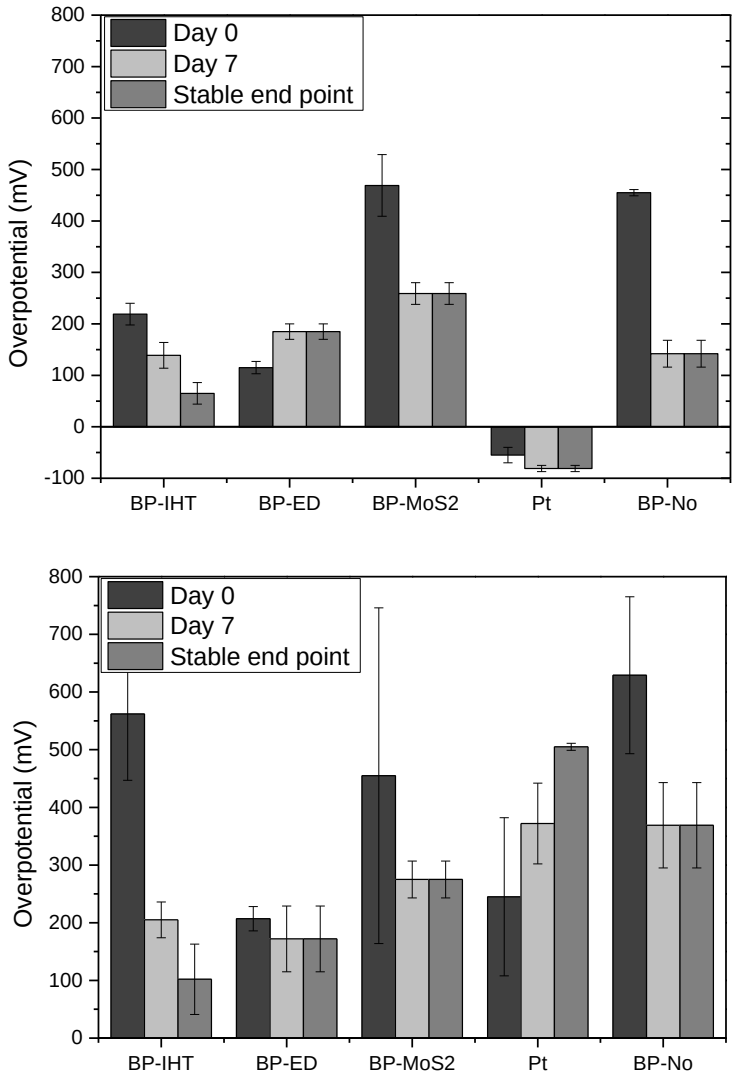

571 **Figure 7** Overpotentials of selected electrodes in long term experiments at reductive current of
572 3 mA cm^{-2} in 0.5 M phosphate buffer (above) and acidic industrial wastewater (below) at
573 different time points. "Stable end point" corresponds to the time where the cathode potential had
574 stabilised ($\Delta E < 5$ mV d^{-1}), which took between 7 and 17 days to reach and is indicated
575 individually above each of the green bars. In each case, standard deviations for three parallel
576 electrolyses are shown.
577

The situation in long term experiments changed dramatically when the same electrochemical runs were carried out in acidic industrial wastewater. Here, the performance of the Pt electrode deteriorated already after some hours as the overpotential increased greatly from 250 ± 140 mV at the start to 510 ± 10 mV after 17 days of continuous electrolysis. Already after 7 days, the Pt cathodes performed worse than all of the investigated MoS_x-based electrodes. After 17 days, the Pt cathodes showed the by far highest overpotential (Fig. 7), even exceeding that of the untreated buckypaper support.

In order to identify a reason for the performance degradation of the Pt electrodes, SEM images of the electrode surfaces were taken both before and after long term electrolyses. These images clearly show the formation of precipitates on the electrode surfaces, which are more pronounced for Pt than for MoS_x electrodes (Fig. 8). It is known that platinum electrodes can be poisoned by various substances (often sulphur compounds [42,43]). This may explain the increasing overpotentials for the Pt electrodes in our industrial wastewater as it contains high concentrations of sulphate (2.0 – 2.8 g L^{-1}) due to the presence of sulphuric acid. At the reducing potentials applied here, SO_4^{2-} could well be reduced to HSO_3^- (E^0 ~ +0.2 V) and further on to elemental sulphur or sulphides. Alternatively, organic material originating from the cellulose –acetate production process could be deposited and/or adsorbed onto Pt from the high loading of organic matter dissolved in the wastewater.

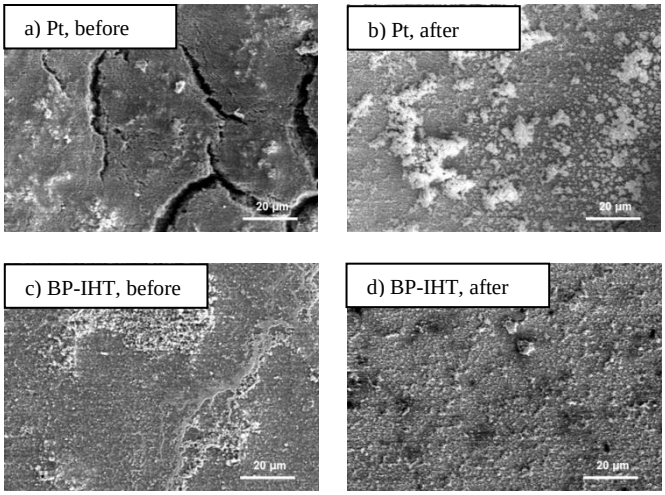

598 **Figure 8** SEM pictures of Pt (a,b) and BP-IHT (c,d) electrodes before use and after long term
599 run in acidic industrial wastewater.

600

601 In contrast to platinum, an opposite trend was found for the MoS_x electrodes, which substantially
602 improved their performance over time. For example, the overpotential for BP-IHT electrodes
603 decreased by nearly half a volt from 560 ± 120 mV to 100 ± 60 mV during 17 days of continuous
604 electrolysis. A possible explanation could be the slow formation of very active, nano-crystalline
605 MoS_2 particles during catalysis. This has recently been reported on the basis of results from high-
606 resolution electron microscopy [44], but a clarification of this issue would require a thorough
607 investigation. Another possibility might be the conversion of MoS_3 to amorphous MoS_2, the
608 latter being known as a better catalyst for HER from previous studies [29]. The conversion of
609 MoS_3 to MoS_2 can occur, for example, by the reduction of sulphur species from the -I to the -II
610 oxidation state, which formally results in the conversion of $Mo^{IV}(S^{2-})_1(S_2^{2-})_1$ to $Mo^{IV}(S^{2-})_2$
611 accompanied by a release of sulphide, e.g. as H_2S. Due to the deposition of various compounds
612 from the wastewater on the electrode surface, this could not be proven here by probing the S :
613 Mo-ratio after the electrolyses by EDX but is definitely an interesting issue for future

614 investigations. The overpotentials of untreated buckypapers also decreased during long term
615 electrolyses both in phosphate buffer and industrial wastewater (Fig. 7). However, the increase
616 was not as large as for MoS_x-coated buckypapers indicating that the improved performance of
617 the MoS_x electrodes was not due to wastewater constituents deposited on the electrodes.
618
619 Overall, these results clearly show that MoS_x electrodes can sustain their high catalytic activity
620 towards HER in real acidic industrial wastewater and that they actually outperform platinum
621 electrodes for H_2 evolution during long term operation. Reasons for this observation might be
622 surface coatings or changes of the MoS_x materials as discussed above. Additionally, it is also
623 possible that this is related to different mechanisms for H_2 formation on Pt versus MoS_x surfaces:
624 for Pt, it has been established that H_2 evolves from hydrogen atoms directly bound to Pt metal
625 centres, while for MoS_x electrodes H_2 formation is thought to occur on the sulphur edges of the
626 MoS_x particles [37]. The mechanistic details of HER on MoS_x are currently much debated in the
627 literature and numerous possible H_2 formation routes are discussed, which e.g. might include
628 Mo^{III}, Mo^{IV} or Mo^{V} ions, H-H bond formation from SH-groups or protonation steps involving
629 Mo-coordinated hydrides [45–50]. In consequence, it seems possible that catalyst inhibitors
630 present in the wastewater (sulphur species, organic matter, etc.) might affect the platinum surface
631 in a very different way than the active sites of MoS_x, which would explain the dramatically
632 different long term stability of HER-electrocatalysts shown in Fig. 6 and 7.
633 Overall, the results of this study indicate the promising potential of MoS_x electrodes for HER in
634 real industrial wastewaters due to 1) lower overpotentials than Pt during long-term operation in
635 practical conditions, and 2) offering a lower-cost solution for Pt.
636

3.6 Hydrogen production

The Faradaic yield for hydrogen production was determined for the two best performing MoS_x-electrodes, BP-ED and BP-IHT, in two chamber electrolysis cells employing Pt mesh as counter electrodes in the anode chambers. Acidic industrial wastewater was continuously pumped through the chamber with a hydraulic retention time of 11.6 h through the chambers to keep the pH stable. The cathodic pH remained under 4.1 during the whole experimental run. The results of headspace gas chromatography measurements showed that H_2 is indeed the main product at the cathode sides with Faradaic H_2 yields (i.e. cathodic hydrogen recoveries) of 90±12% and 91±15% for BP-IHT and BP-ED electrodes, respectively. These hydrogen recoveries are much higher than previously reported for wastewater-fed MEC (16%) [8], but might decrease when the cathodes are combined with biological anodes. H_2 production rates were 0.26 ± 0.03 and 0.39 ± 0.05 $m^3\ m^{-3}\ d^{-1}$ for BP-IHT and BP-ED electrodes with current densities of 1.1 ± 0.1 and 1.7±0.1 mA cm^{-2}, respectively. Similar H_2 production rates were reported for Pt (0.58 $m^3\ m^{-3}$ d) and MoS_2 (0.46 $m^3\ m^{-3}$ d) cathodes in MECs fed with near-neutral industrial wastewaters [27]. On the other hand, the reported rates for stainless steel electrodes in MECs fed with domestic wastewater were much lower (0.007-0.015 $m^3\ m^{-3}$ d) [8,9].

In this study, the MoS_x electrodes prepared with electrodeposition resulted in higher H_2 production rates and cathodic H_2 recoveries than the MoS_x electrodes prepared via impregnation followed by heat treatment. However, the H_2 produced was only collected for the first 7 days. The results of the long term experiment (Fig. 7) indicate that the performance of the BP-IHT would still increase in time. Thus, H_2 production with these electrodes should be studied for even longer time in the future. However, this was beyond the scope of this investigation. In this study, H_2 evolution with MoS_x cathodes was examined with abiotic anodes to better evaluate how the use of acidic industrial wastewater as an electrolyte affects H_2 production. In the future, MoS_x cathodes operated in acidic wastewater will be combined with biological anodes where acetate from the same wastewater is oxidised at neutral pH (also available at the industrial site). Having a pH difference between the anode and cathode should not hinder H_2 evolution in MECs. In fact, Ruiz et al. [2] tested different cathodic pH values with synthetic media and reported the highest H_2 production rates for anodic and cathodic pH values of 7.0 and 2.0, respectively.

673 # 4. Conclusions

674

675 We have demonstrated that MoS_x can clearly outperform platinum as catalyst for H_2 evolution in
676 a real acidic industrial wastewater with regard to long term stability. The best performing MoS_x-
677 electrodes also had lower onset overpotential for H_2 evolution in wastewater (100-130 mV) than
678 stainless steel electrodes (190 mV) which are often used for H_2 production in microbial
679 electrolysis cells at present. In addition, the catalytic activity of the MoS_x electrodes for HER
680 increased in industrial wastewater over time, reaching overpotentials as low as 100 mV (after 17
681 days) at a current density of 3 mA cm^{-2}. The opposite was observed for Pt electrodes where the
682 overpotentials needed to sustain this current density had to be increased from 250 to 510 mV
683 over the same time period. The reasons for the decreasing overpotentials of the MoS_x electrodes
684 need further investigation but might be related to changes in the MoS_x structure and/or the
685 sulphide-to-disulphide (S^{2-} : S_2^{2-}) ratio on the surface of the catalyst. To be able to optimize
686 catalytic performance in a rational way, more mechanistic studies are needed in the future [45–
687 50]. We also found that the MoS_x deposition method as well as the carbon support greatly
688 affected the catalytic activities of the electrodes for HER. Electrodeposition and impregnation
689 followed by heat treatment resulted in lowest overpotentials of the MoS_x electrodes and MoS_x
690 electrodes prepared with these methods resulted in high cathodic H_2 recoveries (around 90%)
691 and H_2 production rates (0.26-0.39 m^3 m^{-3} d). Thus, MoS_x-carbon electrodes offer a viable option
692 for hydrogen evolution in MECs under practical conditions.
693 The possible range of practical application in the field of energy conversion is manifold. As
694 mentioned before, the MoS_x-carbon electrodes are suitable for the application as H_2 evolution
695 cathodes in microbial electrolysis cells treating complex acidic wastewaters, in which platinum

cathodes suffer from severe poisoning. Using the presented MoS_x-cathodes would enable to reduce the total cell voltage of an MEC needed for long-term operation to only 0.5 V, as compared to the approx. 0.9 V required when using the poisoning prone platinum cathodes for longer than a couple of days. This corresponds to an by approx. 40% lower electricity demand for hydrogen production (calculation based on a reasonable operation potential of ~ + 0.4 V vs. RHE for a microbial anode [51] and the cathode operating potentials of ~ – 0.1 V and – 0.5 V vs. RHE after 17 days of operation as displayed in Fig. 6). Furthermore, the new cathodes could also be applied in the emerging field of microbial electrosynthesis [52], were electrical energy is converted into valuable products by hydrogenotrophic microorganisms. Examples are the methanization of CO_2 from biogas [53], and the production of commodities such as acetate or the bioplastic poly-β-hydroxybutyrate from HCO_3^- as carbon source [52]. These energy conversion processes require hydrogen evolution cathodes that are poisoning-resistant in a complex microbial environment. Considering the results of this study, MoS_x might be a very suitable catalyst material for this task. In the light of the energy transition towards an electricity powered world [54], it is expected that microbial electrosynthesis will gain significant future relevance to convert electricity into valuable products [52]. We strongly believe that the bioelectrochemical route can favourably complement the more conventional “Power-to-X”-technologies [55], that are increasingly being researched.

From an application point of view it is particularly important, that the presented electrode fabrication routes can, in principle, be realized at low cost also at larger scale. For example, the carbon-nanotube-based support of the best-performing electrode is fabricated as buckypaper by a simple filtration method similar to paper fabrication. Considering a CNT-loading of 12 g m^{-2} and taking into account the current price of 199 US$ per kg of industrial grade multiwalled-CNTs

(20-40 nm diameter, https://www.cheaptubes.com, accessed on 14.11.2016), its material cost amounts to only 2.38 US$ m^{-2}. Similarly, the investigated MoS_x-deposition methods (drop coating, impregnation and heat treatment, electrodeposition) are feasible at larger scales. With a MoS_x loading of 20 mmol m^{-2} and costs of ~1.5 US$·(mol Mo)$^{-1}$ (http://www.lme.com, accessed on 26.01.2016) the molybdenum costs amount to only 0.03 US$ per m² electrode, resulting in a total material cost of the electrode of only ~2.40 US$ per m². For comparison, just the Pt cost of a 1 m² electrode is already 58 times higher, amounting to 141 US$. (5 mg m^{-2} Pt loading; ~5500 US$·(mol Pt)$^{-1}$, http://www.lme.com, accessed on 26.01.2016). Considering that the MoS_x-cathodes exhibit a four-fold lower overpotential for HER, the results of this study clearly demonstrate the tremendous potential of MoS_x electrodes as efficient and affordable cathodes for HER in real industrial wastewaters.

Acknowledgements

This work was funded by the German Ministry of Education and Research (BMBF) under the program “ERWAS” (Grant No. 02WER1314) and the German Science Foundation (DFG, project KU2885/2-2, part of the priority program SPP1613 *SolarH2*). The authors would also like to thank Joana Madjarov for her help with iR measurements , Alexander Birkenmeier for his assistance in the laboratory, and Zachary Pinder for English proofreading of the manuscript.

References

[1] Hosseini SE, Wahid MA. Hydrogen production from renewable and sustainable energy resources: Promising green energy carrier for clean development. Renewable and Sustainable Energy Reviews 2016;57:850–66.

[2] Ruiz Y, Baeza JA, Guisasola A. Enhanced performance of bioelectrochemical hydrogen production using a pH control strategy 2015;8:389–97.

[3] Kadier A, Kalil MS, Abdeshahian P, Chandrasekhar K, Mohamed A, Azman NF et al. Recent advances and emerging challenges in microbial electrolysis cells (MECs) for microbial production of hydrogen and value-added chemicals. Renewable and Sustainable Energy Reviews 2016;61:501–25.

[4] Li Y, Wang H, Xie L, Liang Y, Hong G, Dai H. MoS2 Nanoparticles Grown on Graphene: An Advanced Catalyst for the Hydrogen Evolution Reaction. J. Am. Chem. Soc. 2011;133(19):7296–9.

[5] Li DJ, Maiti UN, Lim J, Choi DS, Lee WJ, Oh Y et al. Molybdenum Sulfide/N-Doped CNT Forest Hybrid Catalysts for High-Performance Hydrogen Evolution Reaction. Nano Lett 2014;14(3):1228–33.

[6] Logan BE, Call D, Cheng S, Hamelers HVM, Sleutels THJA, Jeremiasse AW et al. Microbial Electrolysis Cells for High Yield Hydrogen Gas Production from Organic Matter. Environmental Science & Technology 2008;42(23):8630–40.

[7] Munoz LD, Erable B, Etcheverry L, Riess J, Basséguy R, Bergel A. Combining phosphate species and stainless steel cathode to enhance hydrogen evolution in microbial electrolysis cell (MEC). Electrochem.Commun. 2010;12(2):183–6.

[8] Heidrich ES, Dolfing J, Scott K, Edwards SR, Jones C, Curtis TP. Production of hydrogen from domestic wastewater in a pilot-scale microbial electrolysis cell. Appl.Microbiol.Biotechnol. 2013;97(15):6979–89.

[9] Heidrich ES, Edwards SR, Dolfing J, Cotterill SE, Curtis TP. Performance of a pilot scale microbial electrolysis cell fed on domestic wastewater at ambient temperatures for a 12 month period. Bioresource Technology 2014;173(0):87–95.

[10] Gil-Carrera L, Escapa A, Mehta P, Santoyo G, Guiot SR, Moran A et al. Microbial electrolysis cell scale-up for combined wastewater treatment and hydrogen production. Bioresource Technology 2013;130(0):584–91.

[11] Gil-Carrera L, Escapa A, Carracedo B, Moran A, Gomez X. Performance of a semi-pilot tubular microbial electrolysis cell (MEC) under several hydraulic retention times and applied voltages. Bioresource Technology 2013;146(0):63–9.

[12] Tokash JC, Logan BE. Electrochemical evaluation of molybdenum disulfide as a catalyst for hydrogen evolution in microbial electrolysis cells. International Journal of Hydrogen Energy 2011;36(16):9439–45.

[13] Ledezma P, Donose BC, Freguia S, Keller J. Oxidised stainless steel: a very effective electrode material for microbial fuel cell bioanodes but at high risk of corrosion. Electrochimica Acta 2015;158:356–60.

[14] Hu H, Fan Y, Liu H. Hydrogen production in single-chamber tubular microbial electrolysis cells using non-precious-metal catalysts. International Journal of Hydrogen Energy 2009;34(20):8535–42.

[15] Selembo PA, Merrill MD, Logan BE. Hydrogen production with nickel powder cathode catalysts in microbial electrolysis cells. International Journal of Hydrogen Energy 2010;35(2):428–37.

[16] Benck JD, Hellstern TR, Kibsgaard J, Chakthranont P, Jaramillo TF. Catalyzing the Hydrogen Evolution Reaction (HER) with Molybdenum Sulfide Nanomaterials. ACS Catal 2014;4(11):3957–71.
[17] Ting LRL, Deng Y, Ma L, Zhang Y, Peterson AA, Yeo BS. Catalytic Activities of Sulfur Atoms in Amorphous Molybdenum Sulfide for the Electrochemical Hydrogen Evolution Reaction. ACS catalysis 2016;6(2):861–7.
[18] He Z, Que W. Molybdenum disulfide nanomaterials: Structures, properties, synthesis and recent progress on hydrogen evolution reaction. Applied Materials Today 2016;3:23–56.
[19] Weber T, Muijsers, J. C., Niemantsverdriet, J. W. Structure of Amorphous MoS3. J. Phys. Chem. 1995;99(22):9194–200.
[20] Laursen AB, Kegnaes S, Dahl S, Chorkendorff I. Molybdenum sulfides-efficient and viable materials for electro - and photoelectrocatalytic hydrogen evolution. Energy Environ. Sci. 2012;5(2):5577–91.
[21] Yuan H, Li J, Yuan C, He Z. Facile Synthesis of MoS 2 @CNT as an Effective Catalyst for Hydrogen Production in Microbial Electrolysis Cells. CHEMELECTROCHEM 2014;1(11):1828–33.
[22] Huang Z, Luo W, Ma L, Yu M, Ren X, He M et al. Dimeric Mo2 S12 (2-) Cluster: A Molecular Analogue of MoS2 Edges for Superior Hydrogen-Evolution Electrocatalysis. Angewandte Chemie (International ed. in English) 2015;54(50):15181–5.
[23] Vrubel H, Hu X. Growth and Activation of an Amorphous Molybdenum Sulfide Hydrogen Evolving Catalyst. ACS Catal 2013;3(9):2002–11.
[24] Pu Z, Liu Q, Asiri AM, Obaid AY, Sun X. Graphene film-confined molybdenum sulfide nanoparticles: Facile one-step electrodeposition preparation and application as a highly active hydrogen evolution reaction electrocatalyst. Journal of Power Sources 2014;263(0):181–5.
[25] Cui W, Liu Q, Xing Z, Asiri AM, Alamry KA, Sun X. MoP nanosheets supported on biomass-derived carbon flake: One-step facile preparation and application as a novel high-active electrocatalyst toward hydrogen evolution reaction. Applied Catalysis B: Environmental 2015;164(0):144–50.
[26] Bian X, Zhu J, Liao L, Scanlon MD, Ge P, Ji C et al. Nanocomposite of MoS2 on ordered mesoporous carbon nanospheres: A highly active catalyst for electrochemical hydrogen evolution. Electrochem.Commun. 2012;22:128–32.
[27] Tenca A, Cusick RD, Schievano A, Oberti R, Logan BE. Evaluation of low cost cathode materials for treatment of industrial and food processing wastewater using microbial electrolysis cells. International Journal of Hydrogen Energy 2013;38(4):1859–65.
[28] Xia X, Zheng Z, Zhang Y, Zhao X, Wang C. Synthesis of MoS2-carbon composites with different morphologies and their application in hydrogen evolution reaction. International Journal of Hydrogen Energy 2014;39(18):9638–50.
[29] Merki D, Fierro S, Vrubel H, Hu X. Amorphous molybdenum sulfide films as catalysts for electrochemical hydrogen production in water. Chem. Sci. 2011;2(7):1262–7.
[30] Yan Y, Ge X, Liu Z, Wang J, Lee J, Wang X. Facile synthesis of low crystalline MoS2 nanosheet-coated CNTs for enhanced hydrogen evolution reaction. Nanoscale 2013;5(17):7768–71.
[31] Balser K, Hoppe L, Eicher T, Wandel M, Astheimer H, Steinmeier H et al. Cellulose Esters. In: Ullmann's Encyclopedia of Industrial Chemistry: Wiley-VCH Verlag GmbH & Co. KGaA; 2000.
[32] Hussein L, Feng YJ, Alonso-Vante N, Urban G, Kr□ger M. Functionalized-carbon nanotube supported electrocatalysts and buckypaper-based biocathodes for glucose fuel cell applications. Electrochim.Acta 2011;56(22):7659–65.

[33] Kipf E, Koch J, Geiger B, Erben J, Richter K, Gescher J et al. Systematic screening of carbon-based anode materials for microbial fuel cells with Shewanella oneidensis MR-1. Bioresource Technology 2013;146(0):386–92.
[34] Zhang X, Luster B, Church A, Muratore C, Voevodin AA, Kohli P et al. Carbon Nanotube−MoS2 Composites as Solid Lubricants. ACS Appl. Mater. Interfaces 2009;1(3):735–9.
[35] Wirth S, Harnisch F, Weinmann M, Schröder U. Comparative study of IVB–VIB transition metal compound electrocatalysts for the hydrogen evolution reaction. Applied Catalysis B: Environmental 2012;126(0):225–30.
[36] Kerzenmacher S, Mutschler K, Kräling U, Baumer H, Ducrée J, Zengerle R et al. A complete testing environment for the automated parallel performance characterization of biofuel cells: design, validation, and application. J.Appl.Electrochem. 2009;39(9):1477–85.
[37] Hinnemann B, Moses PG, Bonde J, Jørgensen KP, Nielsen JH, Horch S et al. Biomimetic Hydrogen Evolution: MoS2 Nanoparticles as Catalyst for Hydrogen Evolution. J.Amer.Chem.Soc. 2005;127(15):5308–9.
[38] Pasupuleti SB, Srikanth S, Venkata Mohan S, Pant D. Development of exoelectrogenic bioanode and study on feasibility of hydrogen production using abiotic VITO-CoRE™ and VITO-CASE™ electrodes in a single chamber microbial electrolysis cell (MEC) at low current densities. Bioresource Technology 2015.
[39] Wang H, Lu Z, Kong D, Sun J, Hymel TM, Cui Y. Electrochemical Tuning of MoS2 Nanoparticles on Three-Dimensional Substrate for Efficient Hydrogen Evolution. Acs Nano 2014;8(5):4940–7.
[40] Lin T, Liu C, Lin J. Facile synthesis of MoS3/carbon nanotube nanocomposite with high catalytic activity toward hydrogen evolution reaction. Applied Catalysis B: Environmental 2013;134–135(0):75–82.
[41] Zhu H, Du M, Zhang M, Zou M, Yang T, Wang S et al. S-rich single-layered MoS2 nanoplates embedded in N-doped carbon nanofibers: efficient co-electrocatalysts for the hydrogen evolution reaction. Chem. Commun. 2014;50(97):15435–8.
[42] Chae KJ, Choi MJ, Kim KY, Ajayi FF, Chang IS, Kim IS. A Solar-Powered Microbial Electrolysis Cell with a Platinum Catalyst-Free Cathode To Produce Hydrogen. Environmental Science & Technology 2009;43(24):9525–30.
[43] Rozendal RA, Hamelers HVM, Rabaey K, Keller J, Buisman CJN. Towards practical implementation of bioelectrochemical wastewater treatment. Trends Biotechnol 2008;26(8):450–9.
[44] Lee SC, Benck JD, Tsai C, Park J, Koh AL, Abild-Pedersen F et al. Chemical and Phase Evolution of Amorphous Molybdenum Sulfide Catalysts for Electrochemical Hydrogen Production. Acs Nano 2016;10(1):624–32.
[45] Deng Y, Ting LRL, Neo PHL, Zhang Y, Peterson AA, Yeo BS. Operando Raman Spectroscopy of Amorphous Molybdenum Sulfide (MoS x) during the Electrochemical Hydrogen Evolution Reaction: Identification of Sulfur Atoms as Catalytically Active Sites for H + Reduction. ACS catalysis 2016;6(11):7790–8.
[46] Ahn HS, Bard AJ. Electrochemical Surface Interrogation of a MoS2 Hydrogen-Evolving Catalyst: In Situ Determination of the Surface Hydride Coverage and the Hydrogen Evolution Kinetics. The journal of physical chemistry letters 2016;7(14):2748–52.

[47] Tang Q, Jiang D. Mechanism of Hydrogen Evolution Reaction on 1T-MoS 2 from First Principles. ACS catalysis 2016;6(8):4953–61.
[48] Zhang N, Li H, Yu K, Zhu Z. Differently structured MoS2 for the hydrogen production application and a mechanism investigation. Journal of Alloys and Compounds 2016;685:65–9.
[49] Tran PD, Tran TV, Orio M, Torelli S, Truong QD, Nayuki K et al. Coordination polymer structure and revisited hydrogen evolution catalytic mechanism for amorphous molybdenum sulfide. Nature Materials 2016;15(6):640–6.
[50] Lassalle-Kaiser B, Merki D, Vrubel H, Gul S, Yachandra VK, Hu X et al. Evidence from in situ X-ray absorption spectroscopy for the involvement of terminal disulfide in the reduction of protons by an amorphous molybdenum sulfide electrocatalyst. J.Amer.Chem.Soc. 2015;137(1):314–21.
[51] Aelterman P, Freguia S, Keller J, Verstraete W, Rabaey K. The anode potential regulates bacterial activity in microbial fuel cells. Appl.Microbiol.Biotechnol. 2008;78(3):409–18.
[52] Rabaey K, Rozendal RA. Microbial electrosynthesis - revisiting the electrical route for microbial production. Nature Reviews Microbiology 2010;8(10):706–16.
[53] Geppert F, Liu D, van Eerten-Jansen M, Weidner E, Buisman C, ter Heijne A. Bioelectrochemical Power-to-Gas: State of the Art and Future Perspectives. Trends in Biotechnology 2016;34(11):879–94.
[54] Armaroli N, Balzani V. Towards an electricity-powered world. Energy Environ.Sci. 2011;4(9):3193.
[55] Foit S, Eichel R, Vinke IC, Haart LGJ de. Power-to-Syngas - an enabling technology for the transition of the energy system? Production of tailored synfuels and chemicals using renewably generated electricity. Angewandte Chemie (International ed. in English) 2016.